



Discovery of a novel series of 4-quinolone JNK inhibitors

Leyi Gong^{a,*}, Yun-Chou Tan^a, Genevieve Boice^a, Sarah Abbot^a, Kristen McCaleb^a, Pravin Iyer^a, Fengrong Zuo^b, Joseph Dal Porto^b, Brian Wong^b, Sue Jin^b, Alice Chang^b, Patricia Tran^b, Gary Hsieh^b, Linghao Niu^b, Ada Shao^c, Deborah Reuter^a, Christine M. Lukacs^d, R. Ursula Kammlott^d, Andreas Kuglstatter^c, David Goldstein^a

^a Department of Medicinal Chemistry, Roche Palo Alto, Palo Alto, CA 94304, USA

^b Inflammation Therapeutic Area, Roche Palo Alto, Palo Alto, CA 94304, USA

^c Department of Discovery Technologies, Roche Palo Alto, Palo Alto, CA 94304, USA

^d Department of Discovery Technologies, Hoffmann-La Roche, Nutley, NJ, USA

ARTICLE INFO

Article history:

Received 6 August 2012

Revised 10 October 2012

Accepted 15 October 2012

Available online 24 October 2012

Keywords:

JNK

JNK inhibitors

4-Quinolone

c-Jun N-terminus kinase

Kinase inhibitors

ABSTRACT

A novel series of highly selective JNK inhibitors based on the 4-quinolone scaffold was designed and synthesized. Structure based drug design was utilized to guide the compound design as well as improvements in the physicochemical properties of the series. Compound (**13c**) has an IC₅₀ of 62/170 nM for JNK1/2, excellent kinase selectivity and impressive efficacy in a rodent asthma model.

Published by Elsevier Ltd.

The c-Jun N-terminal kinases (JNKs) are a family of serine/threonine protein kinases of the mitogen-activated protein kinase (MAPK) group along with p38 and ERK.^{1–3} JNKs can be expressed as 10 different isoforms by mRNA alternative splicing of three highly related genes, JNK1, JNK2 and JNK3.⁴ While JNK1 and JNK2 are found to be ubiquitously expressed, JNK3 is principally present in the brain, cardiac muscle, and testis.⁵ Based on the role of JNK in regulating members of the activator protein-1 (AP-1) transcription factors and other cellular factors implicated in gene expression, cellular survival and proliferation in response to cytokines and growth factors, inhibiting JNK may have many potential therapeutic utilities.^{6,7} Consequently, many chemotypes of JNK inhibitors have been reported in the literature.^{8–19}

JNK plays a critical role in T cell signaling and has been shown to regulate the expression or function of a number of proinflammatory cytokines (TNF α , IL-2, IL-6, etc.), that are central to many human inflammatory disorders.⁶ As such, JNK inhibitors have the potential to be immuno-modulatory agents and are of therapeutic interest for the treatment of rheumatoid arthritis and asthma. Since both JNK1 and JNK2 are implicated, dual JNK1/2 inhibitors are developed.

This manuscript describes our effort to discover a novel and selective class of JNK inhibitors. A high throughput screening campaign of a compound library yielded hits from several distinct chemotypes including the quinazoline-dione (**1**) shown in Figure 1. Although **1** had rather modest potency against JNK1 and 2 enzymes, it exhibited exquisite selectivity against other kinases (only inhibited JNK1/2/3, across a panel of 317 kinases). More elaborate analogs (**2**, **3**) showed a 5- to 8-fold improvement in potency.

Combining the knowledge from early SAR taken together with published reports on JNK inhibitors from Takeda (**4**),^{8,9} a novel series of 4-quinolone JNK inhibitors were derived as exemplified by compound **5**, Figure 1. Initial profiling of several compounds from this series revealed that the molecules suffered from poor physicochemical properties including high lipophilicity, high protein binding, and low solubility. Optimization efforts subsequently focused on reducing the lipophilicity and protein binding while improving intrinsic potency for JNK 1 and JNK2.

Synthesis of these compounds was accomplished as outlined in Schemes 1–3.

4-Quinolone analogs were synthesized starting with commercially available 2-nitro-4-chloro-benzoic acid (**6**). A four step sequence (acid chloride formation, malonate addition, base hydrolysis and de-carboxylation) led to ketone **7**. The nitro group of **7** was reduced to amino analog (**8**) by iron powder, which was further elaborated using copper and PhI to afford diphenylaniline

* Corresponding author. Tel.: +1 650 859 4306; fax: +1 650 859 3153.

E-mail address: leyi.gong@sri.com (L. Gong).

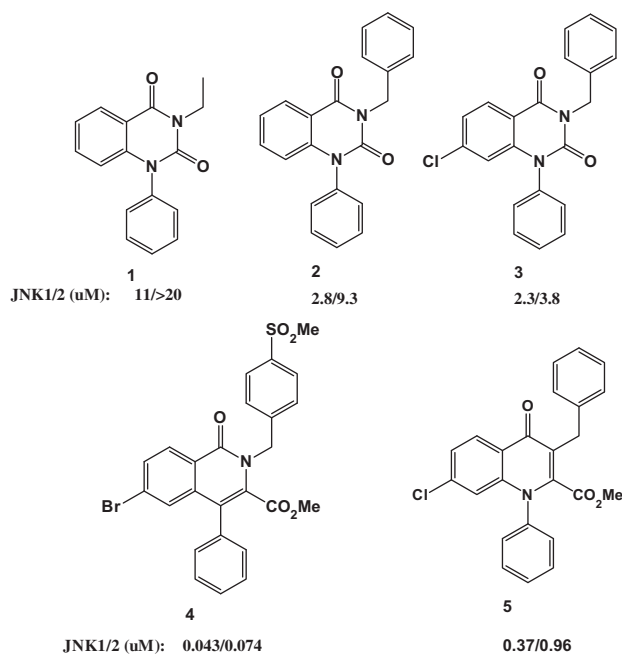


Figure 1. Hit evolution to 4-quinolone.

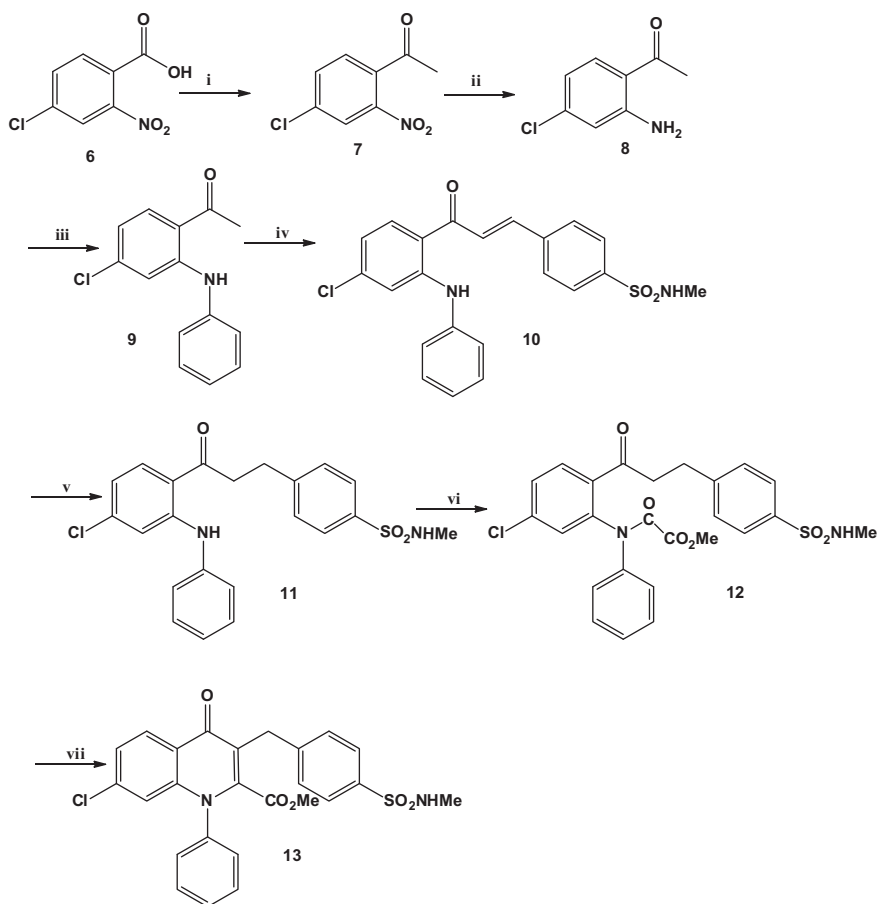
(9). Aldol condensation, dehydration, and reduction gave rise to **10**, then **11**. Reaction of **11** with methyl oxalyl chloride provided intermediate **12**. Without isolation, **12** was heated with a base to give

the final product **13**. Compounds (**13a–f**) were synthesized based on this route.

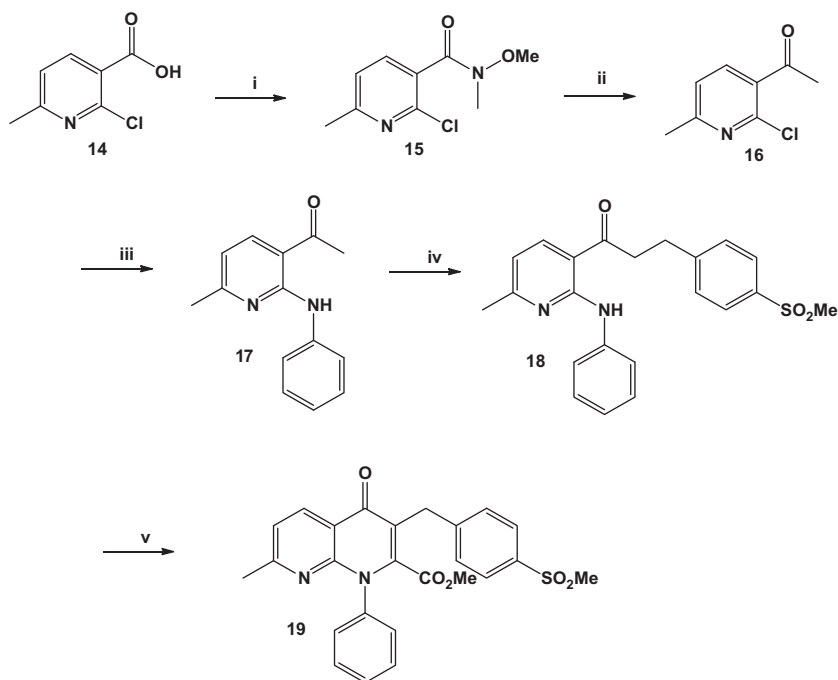
Aza-4-quinolone derivatives were made based on Scheme 2. Weinreb amide (**15**) was made from a substituted nicotinic acid (**14**). The amide (**15**) was further converted to the corresponding ketone (**16**) in good yield. Aniline displacement of **16** gave compound **17**, which underwent aldol condensation and subsequent reduction by hydrogen to afford **18**. Compound **18** was cyclized with ClCOCO₂Me to provide **19a–f**.

Scheme 3 highlights the synthetic route to access benzylic replacement of the 4-quinolone series. Compound **20** can be synthesized using conditions described in Scheme 1, step ii–iii from 4-fluoro-2-nitro benzoic acid. Similarly, Weinreb amide (**21**) was made from **20** and was further converted to α,β -unsaturated vinyl ketone (**22**). Michael addition with 4-methylsulfonyl piperidine afforded **23**, which underwent cyclization with ClCOCO₂Me with a base to give **24a–e**.

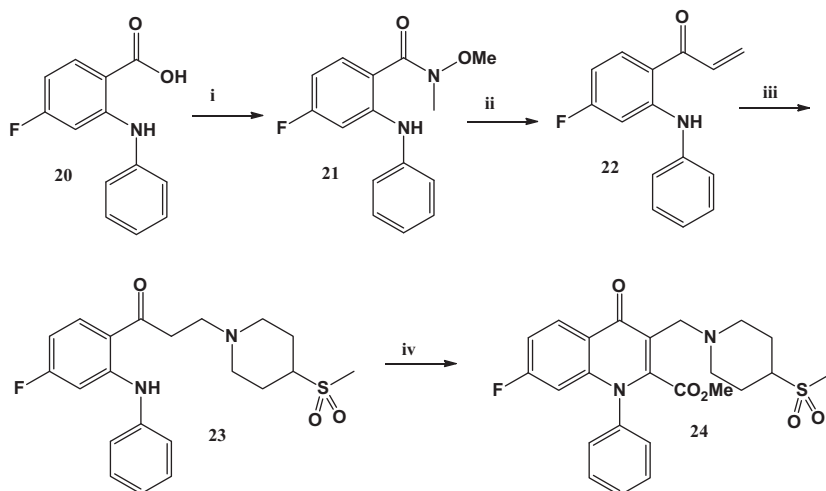
The compounds were evaluated for their ability to inhibit JNK1 and JNK2 using ³³P radiometric assay,²¹ their JNK cellular potency (c-Jun)²² and their propensity to bind to human serum albumin. Results are shown in Tables 1–3. A higher throughput surrogate assay for measuring a compound's affinity for human serum protein was developed. The JNK1 enzyme assay was modified to incorporate 40% human serum albumin and inhibitors were tested for their ability to inhibit JNK1 both in the presence and absence of 40% human serum albumin. Compounds were subsequently ranked to de-prioritize those that lost the most potency in the presence of human serum albumin. Compounds with high protein binding were typically highly lipophilic which often led to poor



Scheme 1. Reagents and conditions: (i) (COCl)₂, NaH/CH(CO₂Et)₂ in THF 50%; (ii) Fe/NH₄Cl in EtOH/H₂O in 98%; (iii) PhI, Cu, KI, K₂CO₃ in butyl ether, 160 °C, overnight, 86%; (iv) 2 equiv 2 N NaOH, 4-MeNHSO₂-PhCHO, in MeOH, overnight, rt 40%. (v) H₂, Pd/C, THF/ethyl acetate (1:1), 95%; (vi) ClCOCO₂Me in toluene, rt, 4 h; (vii) NaHMDS in MeOH, 75%.



Scheme 2. Reagents and conditions: (i) EDCI/NHMe(OMe), 61%; (ii) MeMgCl in THF, 92%; (iii) Pd(OAc)₂/BINAP, PhNH₂, 95%; (iv) 2 N NaOH, 4-MeSO₂-PhCHO, rt in MeOH, overnight, 48%; (v) H₂, Pd on C and ClCOCO₂Me, K₂CO₃ in MeOH, 37%.



Scheme 3. Reagents and conditions: (i) EDCI/NHMe(OMe), 78%; (ii) CH₂=CHMgCl in THF, 84%; (iii) 4-SO₂Me-piperidine, reflux in EtOH, 85%; (iv) (a) ClCOCO₂Me in toluene, rt. (b) NaHMDS in MeOH, 84%.

cellular potency and correlated with poor physicochemical properties such as low aqueous solubility.

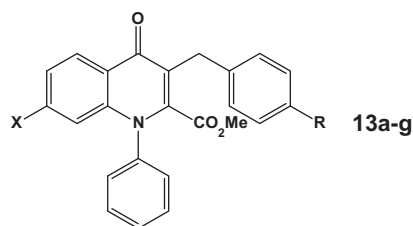
The quinolone series was initially optimized at the 4-position of benzyl ring and 7-position of quinolone as X and R in Table 1. The aim was to reduce the overall lipophilicity while maintaining or improving intrinsic potency for JNK1 and JNK2. Substitution from Br to Cl and F at the 7-position resulted in a significant reduction in lipophilicity, which was reflected in the ratio of enzyme activity of JNK1 in the presence and absence of 40% human serum albumin. Fluoro analogs being less lipophilic and less protein bound had the lowest ratio. Interestingly, the halogen change did not cause a loss of intrinsic potency.

The initial SAR effort and computer modeling supported the binding mode where the quinolone carbonyl oxygen moiety made

a single interaction with Met (111) on the hinge domain in the ATP binding pocket of JNK1. The benzyl group was modeled to optimize lipophilic interactions with the protein. The 4-position of the benzyl group (R) directed out towards solvent exposed region of the protein. This binding mode was later confirmed by the X-ray structure with compound **13g** (Table 2) bound to the JNK1 β (Fig. 2).²⁰ Compound design was primarily guided by this structural information.

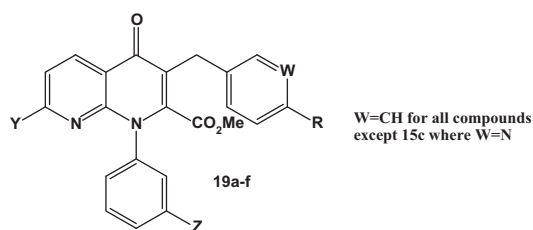
Further evolution of the series was based on combining the common binding motif between the quinolone and reported azaindazoles¹⁶ to give aza-quinolone.

Azaindazole in Figure 3 is AstraZeneca's JNK3 Inhibitor¹⁶ with potency of 0.8 μ M in IC₅₀. Shown in Table 2, the aza-quinolone (**19a-f**) had improved cellular potency as compared to quinolone

Table 1
4-Quinolone analogs

Compds	X	R	JNK1/JNK2 IC ₅₀ , nM ^a	40% HS shift	c-Jun (μM) ^b
4			43/72	110	na
13a	Cl		47/170	20	na
13b	Cl		38/94	26	na
13c	Cl		62/170	22	3.0
13d	Cl		30/50	17	1.0
13e	F		30/70	7.5	1.7
13f	F		50/200	6.8	na
13g	F		58/219	9.1	2.5

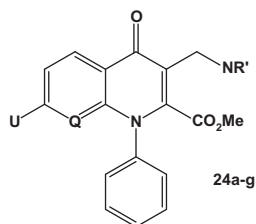
na = no data obtained.

^a Compounds were characterized by mass spectral, ¹H NMR, elemental analysis and mp. IC₅₀ values are an average of multiple determinations ($n \geq 2$). Assay conditions are described in Ref. 21.^b Cellular activity was measured based on the description in Ref. 22.**Table 2**
Aza-quinolone analogs

Compds	Y	Z	R	JNK1/JNK2 IC ₅₀ , nM ^a	40% HS shift	c-Jun (μM) ^b
19a	Me	H		30/64	13	4.2
19b	Me	H		18/28	8.4	0.56
19c	Me	H		45/87	6.8	4.7
19d	Me	NH ₂		14/32	14	0.86
19e	CF ₃	H		82/220	11	2.7
19f	CF ₃	H		80/176	7.9	4.3

^a Compounds were characterized by mass spectral, ¹H NMR, elemental analysis and mp. IC₅₀ values are an average of multiple determinations ($n \geq 2$). Assay conditions are described in Ref. 21.^b Cellular activity was measured based on the description in Ref. 22.

Table 3
Benzyl replacement analogs



Compds	U	Q	NR'	JNK1/JNK2 IC ₅₀ , nM ^a	40% HS shift	c-Jun (μM) ^b
24a	F	CH		65/507	4.5	na
24b	F	CH		23/140	10	0.83
24c	F	CH		114/900	3	na
24d	F	CH		130/1310	3	na
24e	F	CH		53/535	2.4	na
24f	CH ₃	N		na/190	8.3	0.43
24g	CF ₃	N		na/290	3.4	4.3

na = no data obtained.

^a Compounds were characterized by mass spectral, ¹H NMR, elemental analysis and mp. IC₅₀ values are an average of multiple determinations ($n \geq 2$). Assay conditions are described in Ref. 21.

^b Cellular activity was measured based on the description in Ref. 22.

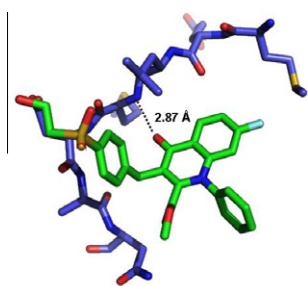


Figure 2. X-ray structure of compound **13g** bound to JNK1β ATP binding pocket.

derivatives shown in Table 1. The addition of the nitrogen, presumably, lowered the lipophilicity, lower serum albumin binding propensity, and lower non-specific binding, thus potent cellular potency.

To further optimize the lipophilic interactions of the series with JNK, the benzyl group was replaced with saturated rings. Shown in Table 3, compound **24a–g** maintained good potency and had reduced protein binding as reflected in the lower shift value in 40% HS shift assay.

Compounds from each sub-class were then characterized in a panel of assays for their physicochemical properties. Shown in Table 4, these compounds demonstrated reasonable solubility, good permeability with no or very modest efflux potential.

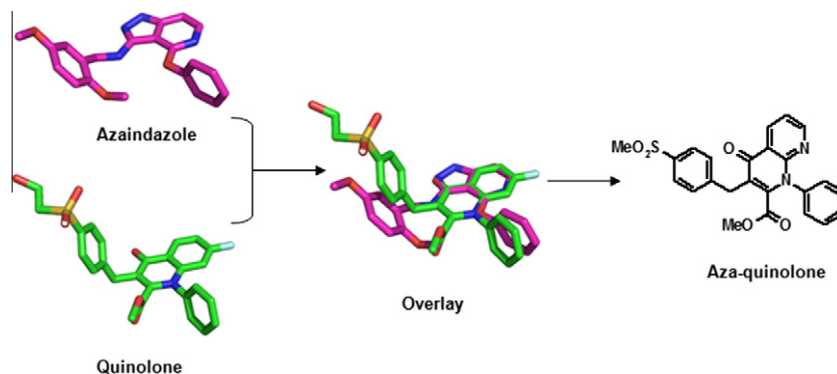


Figure 3. Overlay of quinolone with azaindazole.¹⁶

Table 4
Physicochemical properties

Compds	PSA	Solubility ^a	CACO2 (AB) ^b	ER ^c
13c	80	8.5	2.8	7
13d	83	23	2.4	2
13e	83	37	NA ^d	NA ^d
19a	90	78	1.3	15
24b	74	34	16	2

^a Solubility was measured in a standard PO₄ buffer system with pH of 6.4, unit: µg/mL.

^b unit: ×10⁻⁶ cm/min.

^c ER = AB/BA.

^d NA = not measured.

Table 5
Pharmacokinetic data of **13c**

Species	Route	Cl ^a	T _{1/2} ^b	%F ^c
Rat	IV ^d	25	60	
	PO ^e			6
	PO ^f			43
	IP			100
Dog	IV ^d	3.4	150	
	PO ^e			40

^a Unit: ml/min-kg.

^b Unit: min.

^c Oral bioavailability.

^d Dose: 3 mpk.

^e 3 mpk in hydroxypropyl methylcellulose (HPMC) (suspension).

^f 3 mpk in labrasol (solution).

Table 5 illustrates that compound **13c** had a good balance of potency and properties, and was further characterized in vivo. It showed good oral bioavailability in two species. The in vivo clearance rate of **13c** in rat and dog can be characterized as medium and low, respectively.

The kinase selectivity of **13c** was then evaluated against a commercial panel of 317 kinases.^{23,24} As **Table 6** indicates that **13c** exhibited excellent kinase selectivity with potency observed for only JNK enzymes.

Since compound **13c** exhibited reasonable pharmacokinetics and good kinase selectivity, it was evaluated in a rat asthma model. Ovalbumin-induced allergic asthma is a widely used model to reproduce the airway eosinophilia, pulmonary inflammation and elevated IgE levels associated with the disease.

Results are summarized in **Figure 4**, which shows that compound **13c** when dosed at 10 mg/pk s.c. inhibited neutrophil infiltration in BAL (Bronchial Alveolar Lavage) by 55% at 4hrs post-challenge and inhibited the total white blood cells infiltration in BAL by 40%. These changes correlated with a proportional loss in the relative JNK activity observed in the lung.^{25,26} Results for reduction in airway neutrophil infiltration are comparable to those observed for dexamethasone or p38 inhibitors, such as SB 203580 or LY2228820, in similar studies.

In summary, a potent, selective and novel series of JNK inhibitors was discovered. Structure based drug design was used to optimize not only intrinsic potency, but also the physicochemical properties of the series. Compound **13c** showed significant suppression of inflammatory cell infiltration in the rat asthma model,

Table 6
Kinase selectivity profile of **13c**^b

Kinase	K _d ^a	Kinase	K _d ^a	Kinase	K _d ^a
JNK1	0.062	P38-δ	>10	SgK085	>10
JNK2	0.170	IRAK1	>10	MAPK7	>10
IKK-β	>10	DAPK3	>10	DCAMKL3	>10
p38-γ	>10	MAPK15	>10	RIOK2	>10
STK17A	>10	DAPK2	>10	CDK7	>10
DAPK1	>10	MAP2K4	>10	RPS6KA1	>10

^a K_d of a kinase in µM.

^b The rest of kinases in the panel^{23,24} (unlisted in this table) all have K_d of >10 µM; all K_ds were determined in DiscoverRX.

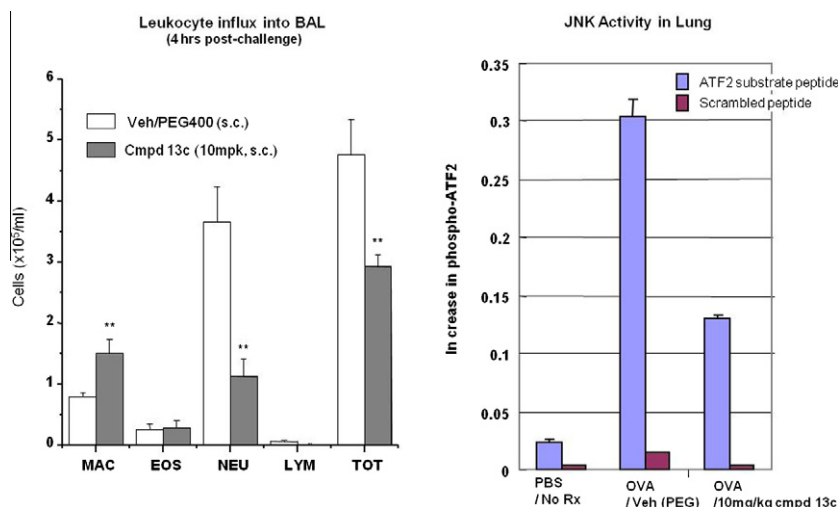


Figure 4. Compound **13c** in rat model of Ova-Induced Lung Hyper-responsiveness. (A) Changes to BAL leukocyte infiltrates at 4 h post intranasal challenge; (B) Relative JNK kinase activity as measured in lung tissue by ex vivo substrate phosphorylation assay.

suggesting that JNK inhibition may be attractive as a novel therapeutic approach for the treatment of asthma.

References and notes

- Derijard, B.; Hibi, M.; Wu, I. H.; Barrett, T.; Su, B.; Deng, T.; Karin, M.; Davis, R. J. *Cell* **1994**, *76*, 1025.
- Kallunki, T.; Su, B.; Tsigelny, I.; Sluss, H. K.; Derijard, B.; Moore, G.; Davis, R.; Karin, M. *Genes Dev.* **1994**, *8*, 2996.
- Kyriakis, J. M.; Avruch, J. *J. Biol. Chem.* **1990**, *265*, 17355.
- Grupta, S.; Barrett, T.; Whitmarsh, A. J.; Cavanagh, J.; Sluss, H. K.; Derijard, B.; Davis, R. J. *EMBO J.* **1996**, *15*, 2760.
- Martin, J. H.; Mohit, A. A.; Miller, C. A. *Mol. Brain Res.* **1996**, *35*, 47.
- Manning, A. M.; Davis, R. J. *Nat. Rev. Drug Discovery* **2003**, *2*, 554.
- Wellen, K. E.; Hotamisligil, G. S. *J. Clin. Invest.* **2005**, *115*, 1111.
- Asano, Y.; Kitamura, S.; Ohra, T.; Aso, K.; Igataa, H.; Tamura, T.; Kawamoto, T.; Tanaka, T.; Sogabe, S.; Matsumoto, S.; Yamaguchi, M.; Kimura, H.; Itoh, F. *Bioorg. Med. Chem.* **2008**, *16*, 4699.
- Asano, Y.; Kitamura, S.; Ohra, T.; Itoh, F.; Kajino, M.; Tamura, T.; Kaneko, M.; Ikeda, S.; Igata, H.; Kawamoto, T.; Sogabe, S.; Matsumoto, S.; Tanaka, T.; Yamaguchi, M.; Kimura, H.; Fukumoto, S. *Bioorg. Med. Chem.* **2008**, *16*, 4715.
- Liu, G.; Zhao, H.; Liu, B. *Bioorg. Med. Chem. Lett.* **2007**, *17*, 495.
- Szczepankiewicz, B. G.; Kosogof, C.; Nelson, L. T.; Liu, G.; Liu, B.; Zhao, H.; Serby, M. D.; Xin, Z.; Liu, M.; Gum, R. J.; Haasch, D. L.; Wang, S.; Clampit, J. E.; Johnson, E. F.; Lubben, T. H.; Stashko, M. A.; Olejniczak, E. T.; Sun, C.; Dorwin, S. A.; Haskins, K.; Abad-Zapatero, C.; Fry, E. H.; Hutchins, C. W.; Sham, H. L.; Rondinone, C. M.; Trevillyan, J. M. *J. Med. Chem.* **2006**, *49*, 3563.
- Zhao, H.; Serby, M. D.; Xin, Z.; Szczepankiewicz, B. G.; Liu, M.; Kosogof, C.; Liu, B.; Nelson, L. T.; Johnson, E. F.; Wang, S.; Pederson, T.; Gum, R. J.; Clampit, J. E.; Haasch, D. L.; Abad-Zapatero, C.; Fry, E. H.; Rondinone, C.; Trevillyan, J. M.; Sham, H. J.; Liu, G. *J. Med. Chem.* **2006**, *49*, 4455.
- Liu, G.; Zhao, H.; Liu, B.; Xin, Z.; Liu, M.; Serby, M. D.; Lubbers, N. L.; Widomski, D. L.; Polakowski, J. S.; Beno, D. W. A.; Trevillyan, J. M.; Sham, H. L. *Bioorg. Med. Chem. Lett.* **2006**, *16*, 5723.
- Christopher, J. A.; Atkinson, F. L.; Bax, B. D.; Brown, M. J.; Champigny, A. C.; Chuang, T. T.; Jones, E. J.; Mosley, J. E.; Musgrave, J. R. *Bioorg. Med. Chem. Lett.* **2009**, *19*, 2230.
- Alam, M.; Beevers, R. E.; Ceska, T.; Davenport, R. J.; Dickson, K. M.; Fortunato, M.; Gowers, L.; Haughan, A. F.; James, L. A.; Jones, M. W.; Kinsella, N.; Lowe, C.; Meissner, J. W. G.; Nicolas, A.; Perry, B. G.; Phillips, D. J.; Pitt, W. R.; Platt, A.; Ratcliffe, A. J.; Sharpe, A.; Tait, L. J. *Bioorg. Med. Chem. Lett.* **2007**, *17*, 3463.
- Stocks, M. J.; Barber, S.; Ford, R.; Leroux, F.; St-Gallay, S.; Teague, S.; Xue, Y. *Bioorg. Med. Chem. Lett.* **2005**, *15*, 3459.
- De, S. K.; Chen, V.; Stebbins, J. L.; Chen, L.; Cellitti, J. F.; Machleidt, T.; Barile, E.; Riel-Mehan, M.; Dahl, R.; Yang, L.; Emdadi, A.; Murphy, R. *Bioorg. Med. Chem. Lett.* **2010**, *18*, 590.
- Kamenecka, T.; Jiang, R.; Song, X.; Duckett, D.; Chen, W.; Ling, Y. Y.; Habel, J.; Laughlin, J. D.; Chambers, J.; Figueroa-Losada, M.; Cameron, M. D.; Lin, L.; Ruiz, C. H.; LoGrasso, P. V. *J. Med. Chem.* **2010**, *53*, 419.
- Noël, R.; Shin, Y.; Song, X.; Koenig, M.; Chen, W.; Ling, Y. Y.; Lin, L.; Ruiz, C. H.; LoGrasso, P.; Cameron, M. D.; Duckett, D. R.; Kamenecka, T. M. *Bioorg. Med. Chem. Lett.* **2011**, *21*, 2732.
- PDB accession number: 4G1W.
- JNK activity was measured by phosphorylation of GST-ATF2 (19-96) with [γ - 33 P] ATP. The enzyme reaction was conducted at K_m concentrations of ATP and the substrate final volume of 40 μ l in buffer containing 25 mM HEPES, pH 7.5, 2 mM dithiothreitol, 150 mM NaCl, 20 mM MgCl₂, 0.001% Tween[®]20, 0.1% BSA and 10% DMSO. Human JNK2 α 2 assay contains 1 nM enzyme, 1 μ M ATF2, 8 μ M ATP with 1 μ Ci [γ - 33 P] ATP. Human JNK1a1 assay contains 2 nM enzyme, 1 μ M ATF2, 6 μ M ATP with 1 μ Ci [γ - 33 P] ATP. The enzyme assay was carried out in the presence or absence of several compound concentrations. JNK and compound were pre-incubated for 10 min, followed by initiation of the enzymatic reaction by adding ATP and the substrate. The reaction mixture was incubated at 30 °C for 30 min. At the end of incubation, the reaction was terminated by transferring 25 μ l of the reaction mixture to 150 μ l of 10% glutathione Sepharose[®] slurry (Amersham #27-4574-01) containing 135 mM EDTA. The reaction product was captured on the affinity resin, and washed on a filtration plate (Millipore, MABVNOB50) with phosphate buffered saline for six times to remove free radionucleotide. The incorporation of 33 P into ATF2 was quantified on a microplate scintillation counter (Packard Topcount). Compound inhibition potency on JNK was measured by IC₅₀ value generated from ten concentration inhibition curves fitted into the 3-parameter model: % inhibition = Maximum/(1 + ([IC₅₀]/[inhibitor])^{5lope}). Data were analyzed on Microsoft Excel for parameter estimation. For details, please see: Gong, L. et al. WO Patent 138340, 2009.
- c-Jun Activation Assay in TNF α -Induced Human Chondrosarcoma SW1353 Cells: SW1353 cells are grown in DMEM (Invitrogen) with 10% fetal bovine serum (Invitrogen), ascorbic acid (15 mg/ml), penicillin (100 U/ml) and streptomycin (100 mg/ml) (Invitrogen). Cells are plated at a density of 8000 cell per well in 100 ml of growth media for 24 h before the compound treatment. Immediately before the treatment, media is replaced with 90 ml of fresh media, then add 10 ml of 10 \times concentrated compound solution and allowed to pre-incubate with cells for 30 min. The vehicle (DMSO) is maintained at a final concentration of 0.5% in all samples. After 30 min, the cells are activated with 10 ng/ml of TNF α (Roche Biochemical) and incubated 20 min at 37 °C in 5% CO₂. Cells are fixed in 4% formaldehyde/PBS and permeabilized with 0.5% Triton-100/PBS (RocheBiochemical.), then were incubated in blocking buffer (2% BSA/PBS) for 1 h. The cell are stained with c-Jun monoclonal antibody (Santa Cruz Biotechnology) for 1 hour and detected with DyLight 488 Goat anti-mouse antibody (Thermo Fisher), nuclei are stained with Hoechst dye (Thermo Fisher). Images are acquired and quantified by ArrayScan reader (Thermo Fisher). The IC₅₀ values are calculated as the concentration of the compound at which the c-Jun intensity was reduced to 50% of the control value using Xlfit in Microsoft Excel program.
- Bamborough, P.; Drewry, D.; Harper, G.; Smith, G. K.; Schneider, K. *J. Med. Chem.* **2008**, *51*, 7898.
- Goldstein, D. M.; Gray, N. S.; Zarrinkar, P. P. *Nat. Rev. Drug Discovery* **2008**, *7*, 391.
- Ovalbumin-induced Asthma in Rat: Male Brown Norway rats were sensitized and boosted with Ovalbumin on days 1 and 8, and exposed by inhalation to an Ova aerosol (5% Ova–50 mg/ml for 30 min on days 15–16). Alum-sensitized, Ova-challenged BN rats and sham-exposed BN rats served as controls (Warheit et al., 2000). The lungs of rats were evaluated by bronchoalveolar lavage, or snapfrozen for JNK activity assessment at several time points (0–72 h) postexposure. The kinase activity of JNK in lung tissue was measured ex vivo using ATF2 substrate oligopeptide phosphorylation. Compound or vehicle control (PEG) was administered once daily at 10 mg/kg (body wt.) 24 h prior to intranasal challenge.
- Warheit, D. B.; Glatt, C. M.; Janney, D. M.; Webb, T. R.; Reed, K. L.; Wiethoff, A. J. *Annals Occupational Hygiene*, **2000**, *46*(suppl 1), 362.